EXHIBIT A185

Free Radical Biology and Medicine 102 (2017) 122–132

Contents lists available at ScienceDirect

Free Radical Biology and Medicine

journal homepage: www.elsevier.com/locate/freeradbiomed

Original article

Specific point mutations in key redox enzymes are associated with chemoresistance in epithelial ovarian cancer

Nicole M. Fletcher[a], Jimmy Belotte[a], Mohammed G. Saed[a], Ira Memaj[a,b,c], Michael P. Diamond[b], Robert T. Morris[c], Ghassan M. Saed[a,*]

[a] Department of Obstetrics and Gynecology, The C.S. Mott Center for Human Growth and Development, Wayne State University School of Medicine, Detroit, MI 48201, USA
[b] Department of Obstetrics and Gynecology, Augusta University, Augusta, GA 30912, USA
[c] Karmanos Cancer Institute, Detroit, MI 48201, USA

ARTICLE INFO

Keywords:
Ovarian cancer
Oxidative stress
Single nucleotide polymorphism
Chemotherapy

ABSTRACT

Oxidative stress plays an important role in the pathophysiology of ovarian cancer. Resistance to chemotherapy presents a significant challenge for ovarian cancer treatment. Specific single nucleotide polymorphisms (SNPs) in key redox enzymes have been associated with ovarian cancer survival and progression. The objective of this study was to determine whether chemotherapy induces point mutations in key redox enzymes that lead to the acquisition of chemoresistance in epithelial ovarian cancer (EOC). Human EOC cell lines and their chemoresistant counterpart were utilized for this study. Specific SNPs in key redox enzymes were analyzed by TaqMan SNP Genotyping. Activities and levels of key redox enzymes were determined by real-time RT-PCR, ELISA and a greiss assay. Point mutations in key redox enzymes were introduced into sensitive EOC cells via the CRISPR/Cas9 system. Cell viability and IC_{50} for cisplatin were determined by the MTT Cell Proliferation Assay. Data was analyzed with SPSS using Student's two-tailed *t*-tests and One-way ANOVA followed by Dunnett's or Tukey's post hoc tests, $p < 0.05$. Here, we demonstrate that chemoresistant EOC cells are characterized by a further enhancement in oxidative stress as compared to sensitive counterparts. Additionally, chemoresistant EOC cells manifested specific point mutations, which are associated with altered enzymatic activity, in key redox enzymes that are not detected in sensitive counterparts. Supplementation of an antioxidant was able to successfully sensitize EOC cells to chemotherapeutics. Causality was established by the induction of these point mutations in sensitive EOC cells, which resulted in a significant increase in the level of chemoresistance. These findings indicate that chemotherapy induces specific point mutations in key redox enzymes that contribute to the acquisition of chemoresistance in EOC cells, highlighting a potential novel mechanism. Identification of targets for chemoresistance with either biomarker and/or screening potential will have a significant impact for the treatment of this disease.

1. Introduction

Epithelial ovarian cancer (EOC) accounts for the majority of all cancers of the ovaries. It can arise from serous, mucinous, or endometrioid cells on the surface epithelium of the ovary or the fallopian tube [1]. Surgical cytoreduction followed by platinum/taxane chemotherapy results in complete clinical response in 50–80% of patients with stage III and IV disease, but most will relapse within 18 months with chemoresistant [2]. Chemoresistance greatly limits the range of possibilities for subsequent treatments, because some tumors become resistant not only to the initial drug but also to new therapeutic agents with different mechanisms of action [2]. Despite significant advances in surgery, radiation therapy, and anticancer treatment, chemotherapy resistance remains a major obstacle to improving a cancer patient's outcome [3]. Moreover, ovarian cancer is known to be associated with germline mutations in the BRCA1 or BRCA2 genes,

Abbreviations: EOC, epithelial ovarian cancer; SNP, single nucleotide polymorphisms; $O_2^{\bullet-}$, superoxide; H_2O_2, hydrogen peroxide; NAD(P)H, nicotinamide adenine dinucleotide phosphate; iNOS, inducible nitric oxide synthase; MPO, myeloperoxidase; SOD, superoxide dismutase; CAT, catalase; GPX, glutathione peroxidase; GSR, glutathione reductase; GSH, glutathione; NO, nitric oxide; TRAIL, tumor necrosis factor receptor apoptosis-inducing ligand; CSC, cancer stem cells; ATCC, American Type Culture Collection; RT-PCR, Real-Time Reverse Transcription Polymerase Chain Reaction; AGTC, Applied Genomics Technology Center

* Corresponding author.
E-mail addresses: nfletche@med.wayne.edu (N.M. Fletcher), jbelotte@med.wayne.edu (J. Belotte), mgsaed@sgu.edu (M.G. Saed), ira.memaj@wayne.edu (I. Memaj), michael.diamond@augusta.edu (M.P. Diamond), rmorris@med.wayne.edu (R.T. Morris), gsaed@med.wayne.edu (G.M. Saed).

http://dx.doi.org/10.1016/j.freeradbiomed.2016.11.028
Received 5 October 2016; Received in revised form 6 November 2016; Accepted 14 November 2016
Available online 25 November 2016

Table 1
SNP characteristics (A) and SNP genotyping (B) of key redox enzymes in sensitive and chemoresistant EOC cells.

A	Gene (RS number)					
	CAT(rs1001179)	*CYBA*(rs4673)	*NOS2*(rs2297518)	*GPX1*(rs3448)	*GSR*(rs1002149)	*SOD2*(rs4880)
MAF	0.123	0.303	0.173	0.176	0.191	0.371
SNP	C-262T	C242T	C2087T	C-1040T	G201T	T47C
Chromosomal Location	11p13	16q24.3	17q11.2	3p21.31	8p12	6q25.3
Amino Acid Switch	Unknown	Tyrosine to Histidine	Serine to Leucine	Unknown	Unknown	Alanine to Valine
Effect on Activity	Decrease	Decrease	Increase	Unknown	Unknown	Decrease

B	*CAT*C-262T	*CYBA*C242T	*NOS2*C2087T	*GPX1*C-1040T	*GSR*G201T	*SOD2*T47C
MDAH-2774 Sensitive	C/C	T/C	C/C	C/T	G/G	T/T
MDAH-2774 Docetaxel Resistant	C/C	T/T	T/T	C/C	G/G	T/C
MDAH-2774 Cisplatin Resistant	C/C	T/T	T/T	C/C	G/G	T/C
SKOV-3 Sensitive	C/C	T/C	C/C	C/T	G/G	T/T
SKOV-3 Docetaxel Resistant	C/C	T/T	T/T	C/C	G/G	T/C
SKOV-3 Cisplatin Resistant	C/C	T/T	T/T	C/C	G/G	T/C

affecting only 20–40% of patients, suggesting the presence of unknown mutations in other genes [4]. Additional genetic variations, many of which have been identified in recent genome-wide association studies, have been hypothesized to act as low to moderate penetrant alleles, which contribute to ovarian cancer risk, as well as other diseases [5,6]. Thus, many believe that most of the genetic component of ovarian cancer risk is attributed to genetic polymorphisms that confer low to moderate risk, such as single nucleotide polymorphisms (SNPs) that result in point mutations in the gene [7]. Non-synonymous SNPs substitute encoded amino acids in proteins, and are more likely to alter the structure, function, and interaction of the protein [8]. Therefore SNPs are good candidates as disease-modifiers and have been associated with an altered cancer risk [8]. In this study, we have selected several SNPs in key oxidant and antioxidant enzymes based on their effect on function or association with cancer (Table 1).

Cancer cells are known to manifest increased aerobic glycolysis (Warburg effect) and high levels of intrinsic oxidative stress [9,10]. Free radicals such as, superoxide ($O_2^{\bullet-}$), hydroxyl radical, hydrogen peroxide (H_2O_2), peroxynitrite and hypohalous acids are generated as a result of oxidative stress by oxidant enzymes such as nicotinamide adenine dinucleotide phosphate (NAD(P)H)-oxidase, inducible nitric oxide synthase (iNOS), and myeloperoxidase (MPO) [11–13]. The redox balance is maintained by enzyme systems that neutralize toxic free radicals including superoxide dismutases (SOD), catalase (CAT) or by glutathione peroxidase (GPX) coupled with glutathione reductase (GSR) [14]. Other important scavengers include thioredoxin coupled with thioredoxin reductase, and glutaredoxin, which utilizes glutathione (GSH) as a substrate [14,15].

Antioxidant enzymes are differentially expressed in various cancers. In particular, GPX expression is reduced in prostate, bladder and in estrogen-negative breast cancer cell lines, while activity is reduced in cancerous kidney tissues but increased in breast cancer tissues [16–18]. Glutathione reductase levels are elevated in lung cancer although differentially expressed in breast and kidney cancerous tissues [19–21]. Additionally, CAT was found to be decreased in breast, bladder, ovarian and lung cancer while increased in brain cancer [22–26]. Recently, an association of a SNP in *CAT* and survival of ovarian cancer patients has been reported [27]. Superoxide dismutase is expressed in lung, colorectal, gastric, ovarian, and breast cancer, while decreased activity and expression have been reported in colorectal carcinomas and pancreatic cancer cells [24,25,28,29].

Additionally, several pro-oxidant enzymes such as iNOS, MPO, and NAD(P)H oxidase are reported to be increased in EOC tissues and cells [13,30–34]. Expression of iNOS and NAD(P)H oxidase has been found in numerous types of malignant tumors including breast, lung, prostate, bladder, colorectal and malignant melanoma while the expression strongly depends on they histological type/grade of the tumor [35,36]. Moreover, it was reported that cisplatin resistant EOC cells exhibited increased expression of iNOS and its associated product, nitrate/nitrite, as well as a decrease in GSR expression, suggesting a shift towards a pro-oxidant state by these cells [37].

In summary, there is substantial evidence to support a key role of oxidative stress in the maintenance of the oncogenic phenotype as well as in the development of chemoresistance in EOC. First, a pro-oxidant state is strongly associated with ovarian cancer and chemoresistant ovarian cancer. Second, specific mutations in key redox enzymes lead to a change in redox enzymatic function. Third, association of SNPs in key redox enzymes with cancer in the general population has been reported. In this study, we demonstrate the role of oxidative stress in the acquisition of chemoresistance and highlight a cause and effect relationship between exposure to chemotherapeutics, development of point mutations in key redox enzymes, and the acquisition of chemoresistance. The importance of these findings are the identification of targets for chemoresistant ovarian cancer as well as the consideration for the addition of key antioxidants in combination with current chemotherapeutic treatment of ovarian cancer.

2. Materials and methods

2.1. Cell lines, media, and cell culture conditions

Human epithelial ovarian cancer (EOC) cell lines, MDAH-2774 (CRL-10303™) and SKOV-3 (HTB-77™), were obtained from American Type Culture Collection (ATCC, Manassas, VA). Cell lines originated from the ascitic fluid of patients with ovarian endometrioid adenocarcinoma. Cell lines were cultured in 100 cm^2 cell culture dishes (Corning Incorporated, Corning, NY) with McCoy's 5A medium (Invitrogen, Carlsbad, CA) supplemented with 100 U/ml penicillin and 100 μg/ml streptomycin and 10% heat-inactivated fetal bovine serum (FBS, Thermofisher Scientific, Waltham, MA) at 37 °C in 5% CO_2. Culture medium was replaced every two days. Once confluent, 2.5×10^6 cells were seeded in a 150 mm dish and allowed to rest for 24 h followed by their respective media replacement and then cell collection 24 h later for protein extraction and isolation of DNA.

2.2. Development of chemoresistance in EOC cells

Chemotherapy resistant cell lines were conferred by exposing parent EOC cell lines, MDAH-2774 and SKOV-3, to continuous culture in media containing stepwise increases in either cisplatin (Sigma Aldrich, St. Louis, MO) or taxotere (Sigma) over a period of six months with a final concentration of 1.5 μM cisplatin or 0.3 μM taxotere. Upon

reaching final concentrations, cells were grown in the absence chemotherapeutic drugs for two weeks followed by replacement of the drug and verification of resistance by the Trypan blue cell viability and MTT Cell Proliferation assays. Doses were selected based on previously published studies [38,39]. Once confluent, cells were prepared as described above.

2.3. Real-time Reverse Transcription Polymerase Chain Reaction (RT-PCR) for CAT, GPX1, GSR, iNOS and SOD3

2.3.1. RNA isolation

Total RNA was extracted from human ovarian cancer cells using the RNeasy Mini Kit (Qiagen, Valencia, CA) according to the protocol provided by the manufacturer.

2.3.2. Reverse transcription

A 20 µl cDNA reaction volume was prepared from 1 µg RNA using the QuantiTect Reverse Transcription Kit (Qiagen), as described by the manufacturer's protocol. Measurement of the amount of RNA and cDNA in each sample was performed using a Nanodrop Spectrophotometer (ThermoFisher Scientific, Waltham, MA). All cDNA was normalized to 1 µg/µl.

2.3.3. Real-time RT-PCR primer design and controls

Optimal oligonucleotide primer pairs for real-time RT-PCR amplification of reverse-transcribed cDNA were selected with the aid of the software program, Beacon Designer (Premier Biosoft Int., Palo Alto, CA). Human oligonucleotide primers, which amplify variable portions of the protein coding regions, are listed in Supplementary Table 1. Standards with known concentrations were designed specifically for β-actin (79 base pairs (bp)), CAT (105 bp), GPX1 (102 bp), GSR (103 bp), iNOS (103 bp), $p22^{phox}$ (82 bp), and SOD2 (89 bp) using the Beacon Designer software, allowing for construction of a standard curve using a tenfold dilution series. An individual standard for each gene of interest provides a method for absolute quantification of your gene in interest.

Real-time RT-PCR was performed with the QuantiTect SYBR Green RT-PCR kit (Qiagen) and a Cepheid 1.2f Detection System (Cepheid, Sunnyvale, CA). Each reaction was 25-µl consisting of, 12.5 µl of 2 x QuantiTect SYBR Green RT-PCR master mix, 1 µl of cDNA template, and 0.2 µM/L each of target-specific primer that was designed to amplify a part of the gene of interest. To quantify each target transcript, a standard curve was constructed using a tenfold dilution series of the standard for the specific gene of interest. The PCR reaction conditions for β-actin, CAT, iNOS, GPX1, GSR, $p22^{phox}$ and SOD2 are as described in Supplementary Table 1. After PCR, a melting curve analysis was performed to demonstrate the specificity of the PCR product as a single peak. A control, which contained all the reaction components except for the template, was included in all experiments.

2.3.4. TaqMan SNP Genotyping Assay

DNA was isolated utilizing the EZ1 DNA Tissue Kit (Qiagen Valencia, CA) for EOC cells according the manufacturer's protocols. The TaqMan® SNP Genotyping Assay Set (Applied Biosystems, Carlsbad, CA) (NCBI dbSNP genome build 37, MAF source 1000 genomes) were used to genotype the SNPs described in Table 1. The Applied Genomics Technology Center (AGTC, Wayne State University, Detroit, MI) performed these assays. Analysis was done utilizing the QuantStudio™ 12 K Flex Real-Time PCR System (Applied Biosystems).

2.3.5. Protein extraction and analysis

Cell lysates were prepared utilizing cell lysis buffer (Cell Signaling Technology, Danvers, MA) supplemented with ProteaseArrest (G-Biosciences, St. Louis, MO). Total protein concentration of cell lysates was measured with the Pierce BCA Protein Assay Kit (Thermo Scientific, Rockford, Illinois) per the manufacturer's protocol.

2.4. CAT ELISA

The Catalase Assay Kit (Cayman Chemical, Ann Arbor, MI) utilizes the peroxidatic function of CAT for determination of enzyme activity and is based on the reaction of the enzyme with methanol in the presence of an optimal concentration of H_2O_2. The assay was performed according to the manufacturer's protocol using 5 µg total protein. Formaldehyde produced is measured spectrophotometrically with Purpald as the chromogen, which is detected at 540 nm.

2.5. GSR ELISA

The Glutathione Reductase Assay Kit (Cayman Chemical) measures GSR activity by determining the rate of NAD(P)H oxidation which s accompanied by a decrease in absorbance at 340 nm. The assay was performed according to the manufacturer's protocol using 7 µg total protein. Absorbance was read once a minute for 8 min and slope was utilized to calculate GSR activity. Since GSR is present at rate limiting concentrations, the rate of decrease in the absorbance at 340 nm is directly proportional to the GSR activity in the sample.

2.6. GPX ELISA

The Glutathione Peroxidase Assay Kit (Cayman Chemical) indirectly measures GPX activity through its reaction with GSR. Oxidized glutathione, produced from the reduction of an organic hydroperoxide by GPX, is recycled to its reduced state by GSR and NAD(P)H. The oxidation of NADPH to NADP+ is accompanied by a decrease in absorbance at 340 nm. The assay was performed according to the manufacturer's protocol using 10–15 µg of total protein. Absorbance was read once a minute for 8 min and slope was utilized to calculate GPX activity. The rate of decrease in the absorbance 340 is directly proportional to the GPX activity in the sample.

2.7. Nitrate/nitrite assay

Detection of iNOS activity via NO levels was performed with the nitrate/nitrite colorimetric assay (Griess assay) was used to measure the levels of stable NO byproducts in EOC cells lines. Nitrate is a stable oxidation product of NO, and its measurement serves as a convenient assay for NO production. Culture media was analyzed for NO by using nitrate/nitrite colorimetric assay kit (Cayman Chemical, Ann Arbor, MI) per the manufacturer's protocol. Nitrate/nitrite was determined at 540 nm using a microplate reader, and the concentration was calculated using nitrate standards.

2.8. SOD ELISA

The Superoxide Dismutase Assay Kit (Cayman Chemical) detects SOD activity by measuring the dismutation of $O_2^{\bullet -}$ generated by xanthine oxidase and hypoxanthine. The standard curve generated using this enzyme provides a means to accurately quantify the activity of all three types of SOD (Cu/Zn-, Mn-, and Fe-SOD). The assay was performed according to the manufacturer's protocol using 0.25 µg total protein. Total SOD was detected at 460 nm. One unit of SOD is defined as the amount of enzyme needed to exhibit 50% dismutation of $O_2^{\bullet -}$.

2.9. Induction of point mutations in EOC cells with CRISPR/Cas9

The CRISPR/Cas9 system utilizes the Cas9 endonuclease to target a specific site of interest such that user-designed oligos act as templates in the CRISPR/Cas9 system and can generate precise single-nucleotide changes in a gene [40]. Oligos were designed per the GeneArt CRISPR Nuclease Vector Kit (ThermoFisher Scientific) protocol for *SOD2*, *CYBA*, and *GPX1* such that the point mutation would represent the chemoresistant EOC cell genotype identified with SNP genotyping. The

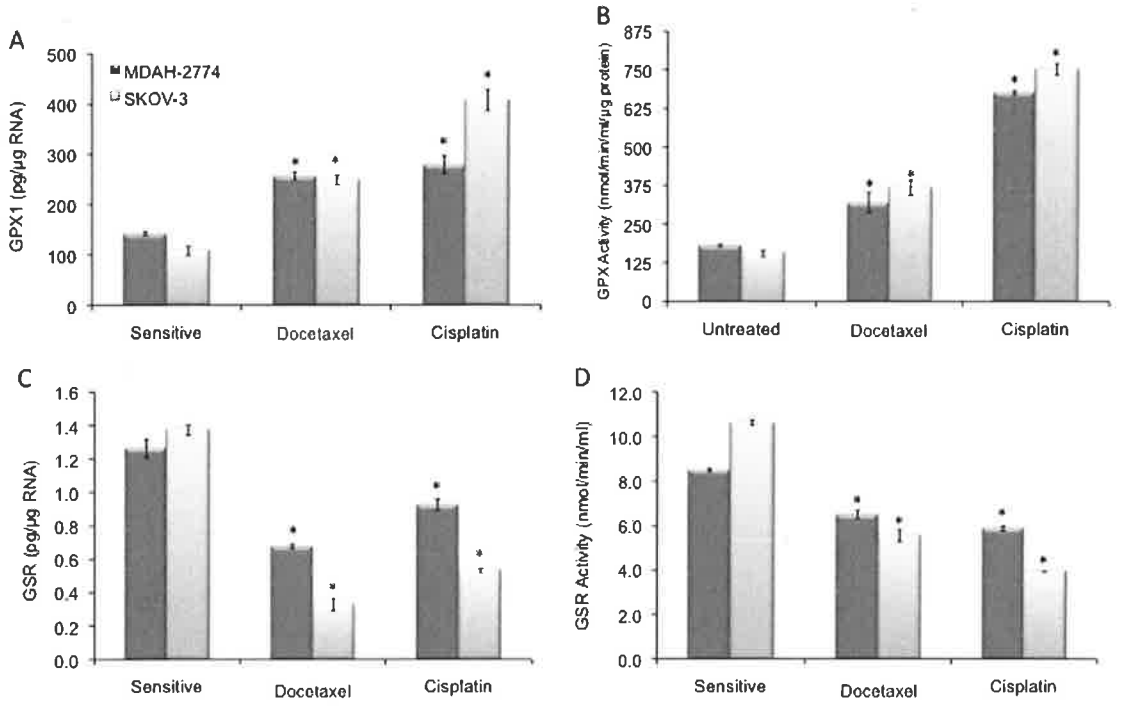

Fig. 1. Alteration of the levels of GPX and GSR in chemoresistant EOC cells. The mRNA and activity levels of GPX (A & B) and GSR (C & D) was determined in EOC cell lines, MDAH-2774 and SKOV-3, and their taxotere or cisplatin resistant counterparts using real-time RT-PCR and ELISA. Experiments were performed in triplicate. Expression is depicted as the mean with error bars representing standard deviation. *$p < 0.05$ as compared to respective sensitive controls.

ds oligo was cloned via a ligation reaction into a CRISPR vector. Cloning of the CRISPR vector was performed in chemically competent *E. coli* included in the kit. Transformed *E. coli* were transferred onto Luria broth (LB) agar plates containing 100 µg/ml ampicillin and grown overnight resulting in ampicillin-resistant colony formation. A single colony was selected and then grown in LB medium containing 100 µg/ml ampicillin overnight and transformed plasmids were subsequently purified with the PureLink HiPure Plasmid Maxiprep Kit (ThermoFisher Scientific) per the manufacturer's protocol. For transfection of the plasmid into our EOC cells, cells were plated (400,000) in a 6-well dish and allowed to grow overnight, to achieve ~80% confluency. 250 µl of Opti-MeM (Life Technologies) was used for transfection and included the specific concentration of the CRISPR vector in a 1:3 ratio of the TransIT-X2 transfection reagent (Mirus Biologicals, Madison, WI). The cells were incubated for 24 h and the presence of fluorescence served as confirmation of transfection of the cells as the CRISPR system contains an orange fluorescence protein reporter. Point mutation induced cells were isolated via cell sorting at the Wayne State University Microscopy, Imaging, and Cytometry (MICR) Resources Core. Cells expressing the orange fluorescent protein were sorted on a Sony SY3200 cell sorter equipped with 355 nm, 405 nm, 488 nm, 561 nm, and 642 nm lasers (Sony Biotechnology, San Jose, CA). Positive cells were then plated in 60 mm2 culture dishes for expansion. The point mutation induced cells were then utilized for assessment of IC_{50} for cisplatin by regression analysis.

2.10. Determination of cell viability, IC_{50} and combination index analysis

Viability was determined using the TACS MTT Cell Proliferation Assay (Trevigen) per the manufacturer's protocol, and as described [41]. A standard curve was constructed using each respective cell line. Cells were seeded into Falcon tissue culture treated 96-well plates in a fixed volume of 100 µl at a density of 8000 cells/well. Cells were treated with increasing doses of either taxotere (0, 0.1, 0.3, 0.6, 1.0, 2.0 3.0, 4.0 µM, VWR Scientific) or cisplatin (0, 0.4, 0.6, 0.8, 1.0, 2.0, 3.0, 4.0 µM, VWR Scientific) with or without SOD (10 U/ml, Sigma-Aldrich) for 24 h. Data was analyzed with regression analysis. For the combination index analysis, dose-effect curve parameters for chemothereapeutics (taxotere or cisplatin) and SOD (10 U/ml) were used for the automated calculation of combination index values conducted by the CompuSyn software (ComboSyn, Paramus, NJ, USA) as previously described [42]. A combination index method that provides qualitative information on the nature of compound interaction (antagonistic, additive or synergistic effect) was used to analyze the results [43]. Fa-combination index plots (Chou-Talalay plots) were generated by the Compusyn Softweare where Fa is the fraction affected (Fa = percentage of inhibition relative to vehicle control/100).

3. Statistical analysis

Data were analyzed using SPSS 22.0 for Windows with independent sample *t*-tests for sensitive EOC cells as compared to their chemoresistant counterparts for ELISAs and real-time RT-PCR. For each MTT viability assay, a chemotherapy or chemotherapy plus SOD dose-response curve was generated in the form of a scatter plot with a linear regression line. The predicted IC_{50} value was determined using a regression equation. Comparisons between cell lines were done using the predicted IC_{50} values and confidence intervals. Statistical significance of $p < 0.05$ is considered significant for all analyses.

4. Results

4.1. Chemoresistant EOC cells manifested a genotype switch in GPX1 as well as an increase in GPX levels as compared to their chemosensitive counterparts

Taxotere resistance resulted in an increase in GPX1 mRNA levels in MDAH-2774 (from 142.0 ± 4.1 to 256.3 ± 7.9 fg/µg RNA, $p < 0.05$) and

in SKOV-3 (from 107.8 ± 8.5 to 247.9 ± 9.5 fg/μg RNA, $p < 0.05$ as compared to their chemosensitive controls (Fig. 1). Additionally, cisplatin resistance resulted in a similar increase in GPX1 mRNA levels in MDAH-2774 (to 279.2 ± 17.4 fg/μg RNA, $p < 0.05$) and in SKOV-3 (to 407.8 ± 20.3 fg/μg RNA, $p < 0.05$) as compared to their chemosensitive controls (Fig. 1).

Taxotere resistance resulted in similar increase in GPX activity levels in MDAH-2774 (from 181 ± 4.5 to 319 ± 31.5 nmol/min/ml/μg protein, $p < 0.05$) and in SKOV-3 (from 155 ± 9.9 to 366 ± 24.9 nmol/min/ml/μg protein, $p < 0.05$) as compared to their chemosensitive controls (Fig. 1). Additionally, cisplatin resistance resulted in a similar increase in GPX activity levels in MDAH-2774 (to 676 ± 5.3 nmol/min/ml/μg protein, $p < 0.05$) and in SKOV-3 (to 751 ± 17.7 nmol/min/ml/μg protein, $p < 0.05$) as compared to their chemosensitive controls (Fig. 1). Sensitive EOC cell lines, MDAH-2774 and SKOV-3, had a SNP genotype for *GPX1* (C/T) that was switched to the common C/C genotype in their chemoresistant counterparts (Table 1B).

4.2. Chemoresistant EOC cells are characterized by decreased GSR levels as compared to their chemosensitive counterparts

Taxotere resistance resulted in a decrease in GSR mRNA levels in MDAH-2774 (from 1.26 ± 0.05 to 0.068 ± 0.01 fg/μg RNA, $p < 0.05$) and in SKOV-3 (from 1.37 ± 0.03 to 0.33 ± 0.03 fg/μg RNA, $p < 0.05$) as compared to their chemosensitive controls (Fig. 2). Additionally, cisplatin resistance resulted in a similar decrease in SOD3 mRNA levels in MDAH-2774 (to 0.92 ± 0.03 fg/μg RNA, $p < 0.05$) and in SKOV-3 (to 0.053 ± 0.01 fg/μg RNA, $p < 0.05$) as compared to their chemosensitive controls (Fig. 2).

Taxotere resistance resulted in a decrease in GSR activity in MDAH-2774 (from 8.5 ± 0.07 to 6.5 ± 0.1 nmol/min/ml, $p < 0.05$) and in SKOV-3 (from 10.6 ± 0.1 to 5.6 ± 0.3 nmol/min/ml, $p < 0.05$) as compared to their chemosensitive controls (Fig. 2). Moreover, cisplatin resistance resulted in a decrease in GSR activity in MDAH-2774 (to 5.9 ± 0.3 nmol/min/ml, $p < 0.05$) and in SKOV-3 (to 3.9 ± 0.0 nmol/min/ml, $p < 0.05$) as compared to their chemosensitive controls (Fig. 2). There was no genotype switch observed for this SNP in *GSR* (Table 1).

4.3. Chemoresistant EOC cells are characterized by a genotype switch in NOS2 as well as increased iNOS and nitrate/nitrite levels as compared to their chemosensitive counterparts

Taxotere resistance resulted in an increase in iNOS mRNA levels in MDAH-2774 (from 374 ± 20.5 to 1530 ± 159 pg/μg RNA, $p < 0.05$) and in SKOV-3 (from 366 ± 32.7 to 1723 ± 26.5 pg/μg RNA, $p < 0.05$) as compared to their chemosensitive controls (Fig. 2). Additionally, cisplatin resistance resulted in a similar increase in iNOS mRNA levels in MDAH-2774 (to 916 ± 96.0 pg/μg RNA, $p < 0.05$) and in SKOV-3 (to 597 ± 13.3 pg/μg RNA, $p < 0.05$) as compared to their chemosensitive controls (Fig. 2).

Taxotere resistance resulted in an increase in nitrate/nitrite levels in MDAH-2774 (from 6.87 ± 0.16 to 8.30 ± 0.18 μM Nitrate/μl media, $p < 0.05$) and in SKOV-3 (from 8.19 ± 0.00 to 16.04 ± 0.36 μM Nitrate/μl media, $p < 0.05$) as compared to their chemosensitive controls (Fig. 2). Moreover, cisplatin resistance also resulted in an increase in nitrate/nitrite levels in MDAH-2774 (to 11.04 ± 0.06 μM Nitrate/μl media, $p < 0.05$) and in SKOV-3 (to 13.74 ± 0.16 μM Nitrate/μl media, $p < 0.05$) as compared to their chemosensitive controls (Fig. 2). The observed increase in nitrate/nitrite, an indirect indicator of iNOS activity, was associated with a genotype switch from common C/C genotype in *NOS2* in sensitive EOC cells to the SNP genotype, T/T, in chemoresistant EOC cells (Table 1).

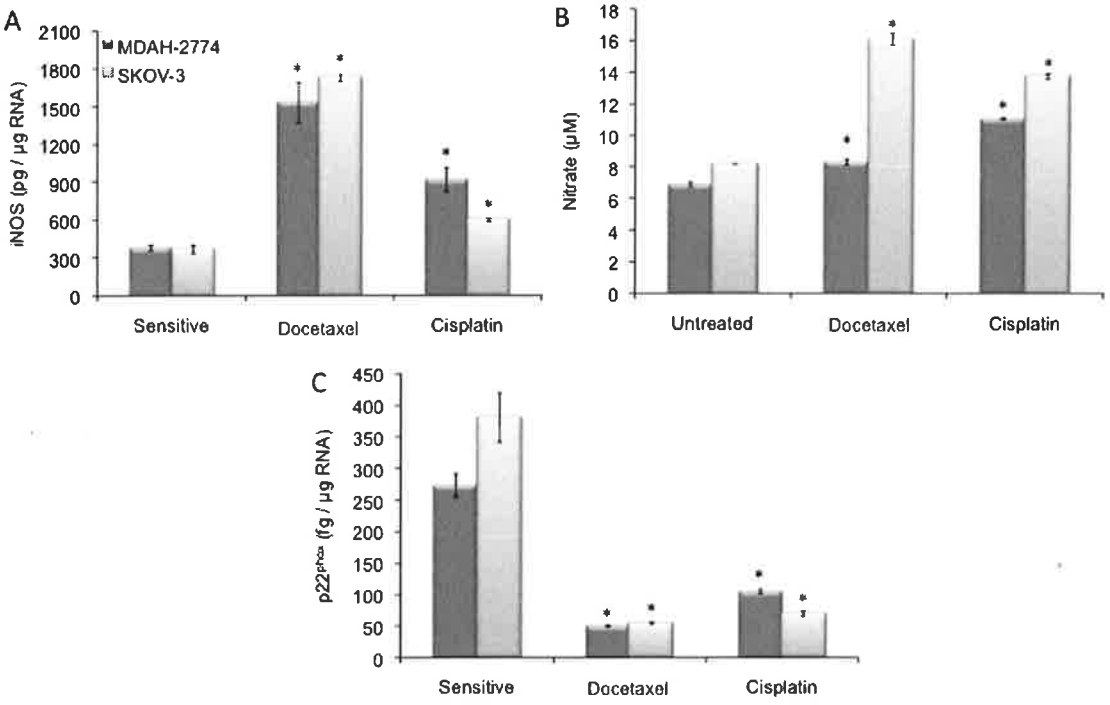

Fig. 2. Alteration of the levels of iNOS, nitrate/nitrite, and p22^{phox} in chemoresistant EOC cells. The EOC cell lines, MDAH-2774 and SKOV-3, and their taxotere or cisplatin resistant counterparts were utilized. The mRNA level of iNOS and p22^{phox} (A & C) were determined by real-time RT-PCR. The level of nitrate/nitrite, a surrogate for NO, was determined by the nitrate/nitrite colorimetric assay (B). Experiments were performed in triplicate. Expression is depicted as the mean and with error bars representing standard deviation. *$p < 0.05$ as compared to respective sensitive controls.

4.4. Chemoresistant EOC cells are characterized by a genotype switch in CYBA *as well as decreased CYBA levels as compared to their chemosensitive counterparts*

Taxotere resistance resulted in a decrease in CYBA (as represented by $p22^{phox}$) mRNA levels in MDAH-2774 (from 272.8 ± 18.4 to 50.5 ± 1.4 fg/μg RNA, $p < 0.05$) and in SKOV-3 (from 380.4 ± 38.6 to 54.5 ± 1.6 fg/μg RNA, $p < 0.05$) as compared to their chemosensitive controls (Fig. 2). Additionally, cisplatin resistance resulted in a similar decrease in $p22^{phox}$ mRNA levels in MDAH-2774 (to 104.7 ± 3.6 fg/μg RNA, $p < 0.05$) and in SKOV-3 (to 70.1 ± 4.3 fg/μg RNA, $p < 0.05$) as compared to their chemosensitive controls (Fig. 2). The observed decrease in $p22^{phox}$ mRNA levels was associated with a genotype switch from the C/T genotype in *CYBA* in sensitive EOC cells to the SNP genotype, T/T, in chemoresistant EOC cells (Table 1).

4.5. Chemoresistant EOC cells are characterized by a genotype switch in SOD2 *as well as a decrease in SOD levels and as compared to their chemosensitive counterparts*

Taxotere resistance resulted in a no statistical difference in SOD2 mRNA levels in MDAH-2774 (from 1.5 ± 0.05 to 1.4 ± 0.02 pg/μg RNA) or in SKOV-3 (from 1.7 ± 0.03 to 1.7 ± 0.2 pg/μg RNA) as compared to their chemosensitive controls (Fig. 3). Additionally, cisplatin resistance also resulted in no statistical difference in SOD2 mRNA levels in MDAH-2774 (to 1.6 ± 0.1 pg/μg RNA) or in SKOV-3 (to 2.2 ± 0.2 pg/μg RNA) as compared to their chemosensitive controls (Fig. 3).

Taxotere resistance resulted in a decrease in SOD activity in MDAH-2774 (from 30111 ± 388 to 18893 ± 490 nmol/min/ml, $p < 0.05$) and in SKOV-3 (from 40373 ± 809 to 24080 ± 2819 nmol/min/ml, $p < 0.05$) as compared to their chemosensitive controls (Fig. 3). Moreover, cisplatin resistance resulted in a similar decrease in SOD activity in MDAH-2774 (to 26960 ± 1011 nmol/min/ml, $p < 0.05$) and in SKOV-3 (to 27956 ± 1600 nmol/min/ml, $p < 0.05$) as compared to their chemosensitive controls (Fig. 3). The observed change in activity was associated with a genotype switch in *SOD2* from the common T/T genotype in sensitive EOC cells to the SNP genotype, T/C, in chemoresistant EOC cells (Table 1).

4.6. Chemoresistant EOC cells are characterized by increased CAT levels as compared to their chemosensitive counterparts

Taxotere resistance resulted in an increase in CAT mRNA levels in MDAH-2774 (from 1.35 ± 0.3 to 2.39 ± 0.2 fg/μg RNA, $p < 0.05$) and in SKOV-3 (from 1.13 ± 0.2 to 1.98 ± 0.2 fg/μg RNA, $p < 0.05$) as compared to their chemosensitive controls (Fig. 3). Additionally, cisplatin resistance resulted in a similar decrease in SOD3 mRNA levels in MDAH-2774 (to 2.5 ± 0.1 fg/μg RNA, $p < 0.05$) and in SKOV-3 (to 1.96 ± 0.2 fg/μg RNA, $p < 0.05$) as compared to their chemosensitive controls (Fig. 3).

Taxotere resistance resulted in an increase in CAT activity in MDAH-2774 (from 6156 ± 213 to 8865 ± 336 nmol/min/ml, $p < 0.05$) and in SKOV-3 (from 6035 ± 487 to 9085 ±131 nmol/min/ml, $p < 0.05$) as compared to their chemosensitive controls (Fig. 3). Moreover, cisplatin resistance also resulted in an increase in CAT activity in MDAH-2774 (to 8823 ± 257 nmol/min/ml, $p < 0.05$) and in SKOV-3 (to 7884 ± 139 nmol/min/ml, $p < 0.05$) as compared to their chemosensitive controls (Fig. 3). There was no observed genotype switch for this SNP in *CAT* (Table 1).

4.7. Induction of a point mutation in SOD2 *or* GPX1 *in sensitive EOC cells resulted in the acquisition of chemoresistance*

A point mutation corresponding to the SNP genotype of chemoresistant SKOV-3 cells was induced in sensitive SKOV-3 cells. These *SOD2* point mutation-induced sensitive cells had a cisplatin IC_{50} of 2.79 (95% CI [2.77–2.80]) compared to 1.87 (95% CI [1.83–1.91]) for their control cells ($p < 0.05$), indicating that the introduction of the point mutation corresponding to the genotype of the chemoresistant

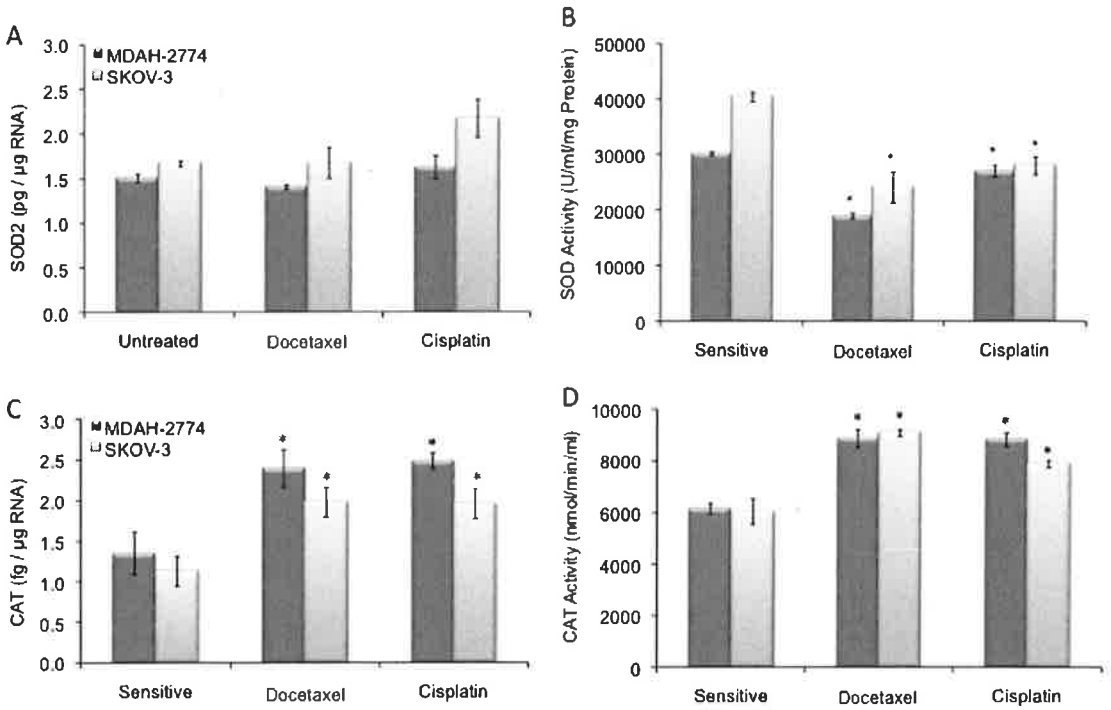

Fig. 3. Alteration of the levels of SOD and CAT in chemoresistant EOC cells. The mRNA and activity levels of SOD2 (A & B) and CAT (C & D) was determined in EOC cell lines, MDAH-2774 and SKOV-3, and their taxotere or cisplatin resistant counterparts using real-time RT-PCR and ELISA. Experiments were performed in triplicate. Expression is depicted as the mean and with error bars representing standard deviation. *$p < 0.05$ as compared to respective sensitive controls.

A

SKOV-3 EOC Cells	Predicted IC_{50}	95% CI min	95% CI max	p-value
Sensitive	1.87	1.83	1.91	< 0.05
Cisplatin Resistant	3.31	3.27	3.35	< 0.05

B

Point Mutations Induced in SKOV-3 EOC Cells	Predicted IC_{50}	95% CI min	95% CI max	p-value
CYBA	1.73	1.70	1.77	< 0.05
GPX1	3.60	3.58	3.62	< 0.05
SOD2	2.79	2.77	2.80	< 0.05

C

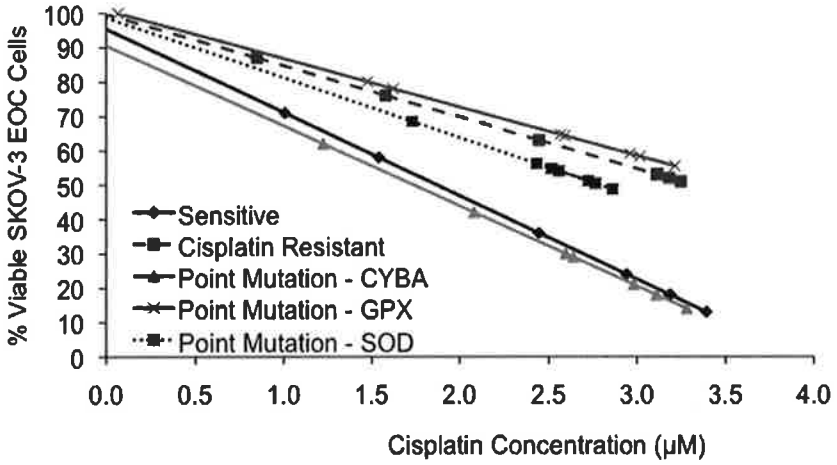

Fig. 4. Induction of point mutations in key redox enzymes in sensitive EOC cells altered the IC_{50} of cisplatin. Point mutations in *SOD2*, *GPX1*, and *CYBA* that were present in the cisplatin resistant SKOV-3 cell line were generated in sensitive cells by the CRISPR/Cas9 system. The Vybrant MTT Cytotoxicity Assay was utilized to predict the IC_{50} using regression analysis (A). 95% Confidence Intervals are listed for each mutation that was generated (B). A plot of the regression lines showing a shift in the IC_{50} due to the induced point-mutation is also depicted (C). Experiments were performed in triplicate. All $p < 0.05$.

EOC cells rendered the cells increasingly resistant to cisplatin by a 0.49-fold change (Fig. 4). Similarly, *GPX1* point mutation-induced sensitive cells had a cisplatin IC_{50} of 3.60 (95% CI [3.58–3.62]) compared to 1.87 (95% CI [1.83–1.91]) for their control cells ($p < 0.05$), indicating that the introduction of the point mutation corresponding to the genotype of the chemoresistant EOC cells rendered the cells increasingly resistant to cisplatin by a 0.92-fold change (Fig. 4). Interestingly, the *CYBA* point mutation-induced sensitive cells resulted in a cisplatin IC_{50} of 1.73 (95% CI [1.70–1.77]) compared to 1.87 (95% CI [1.83–1.91]) for their control cells ($p < 0.05$), indicating that the introduction of the point mutation corresponding to the genotype of the chemoresistant EOC cells sensitized the cells to cisplatin, by a -0.08-fold change (Fig. 4).

4.8. The combination of SOD with chemotherapy significantly increased the efficacy of the chemotherapeutics in EOC cells

The combination of SOD with either taxotere or cisplatin led to a synergistic inhibition of MDAH-2774 cell viability after 24 h in both sensitive and chemoresistant cells (Fig. 5). There was no effect observed following treatment with SOD (10 U/ml) alone. There was an overall shift in the IC_{50} towards a lower dose of chemotherapy when treating the sensitive or the resistant EOC cell line with taxotere or cisplatin in the presence of SOD as compared to the chemotherapy alone ($p < 0.05$, Fig. 6).

5. Discussion

We have previously reported that EOC cells manifest a pro-oxidant state characterized by increased key oxidant enzymes with concomitant decreased antioxidant enzymes [12]. In this study, we have shown that taxotere or cisplatin resistant EOC cells manifest an alteration in the redox balance, further advancing this pro-oxidant environment. Indeed, there was a significant increase in levels of CAT, GPX, and iNOS in chemoresistant EOC cells as compared to their sensitive counterparts (Figs. 1–3). In contrast, there was a decrease in levels in GSR, SOD, and the NAD(P)H oxidase subunit ($p22^{phox}$) (Figs. 1–3). This data supports an important role for an altered redox balance not only in the maintenance of the oncogenic phenotype but also in the development of chemoresistance.

In an attempt to understand the underlying mechanisms of this alteration in the redox balance, we determined the presence of SNPs in key redox enzymes in sensitive and chemoresistant EOC cells. These SNPs were selected based on their ability to change enzymatic activity and/or their association with cancer (Table 1). Chemoresistant EOC cells, and not their sensitive counterparts, manifested specific SNPs in *SOD2*, *NOS2*, and *CYBA* while not in *GSR*, *GPX1* or *CAT*. Interestingly, taxotere and cisplatin chemoresistance conferred an altered activity in CAT and GSR without a change in this specific SNP, as compared to chemosensitive counterparts, indicating possible involvement of other functional SNPs for these enzymes (Table 1, Figs. 1–3). These findings were surprising as we expected the SNPs to be present in both sensitive and chemoresistant cells, since they were derived from the same individual. Thus, our findings imply that chemotherapy can induce point mutations that happen to correspond to change of function SNPs. This data suggests that induction of specific point mutations in sensitive EOC cells corresponding to functional SNPs found in chemoresistant EOC cells directly altered levels of chemoresistance. Therefore, chemotherapy-induced point mutations may lead to the acquisition of chemoresistance in EOC cells.

To determine a cause and effect relationship between point mutations in key redox enzymes and the acquisition of chemoresistance, we have introduced point mutations in sensitive EOC cells followed by evaluation of chemoresistance. We observed a switch at position 47 from T to C in *SOD* in chemoresistant as compared to sensitive cells (Table 1). Utilizing the CRISPR/Cas9 method, we introduced this

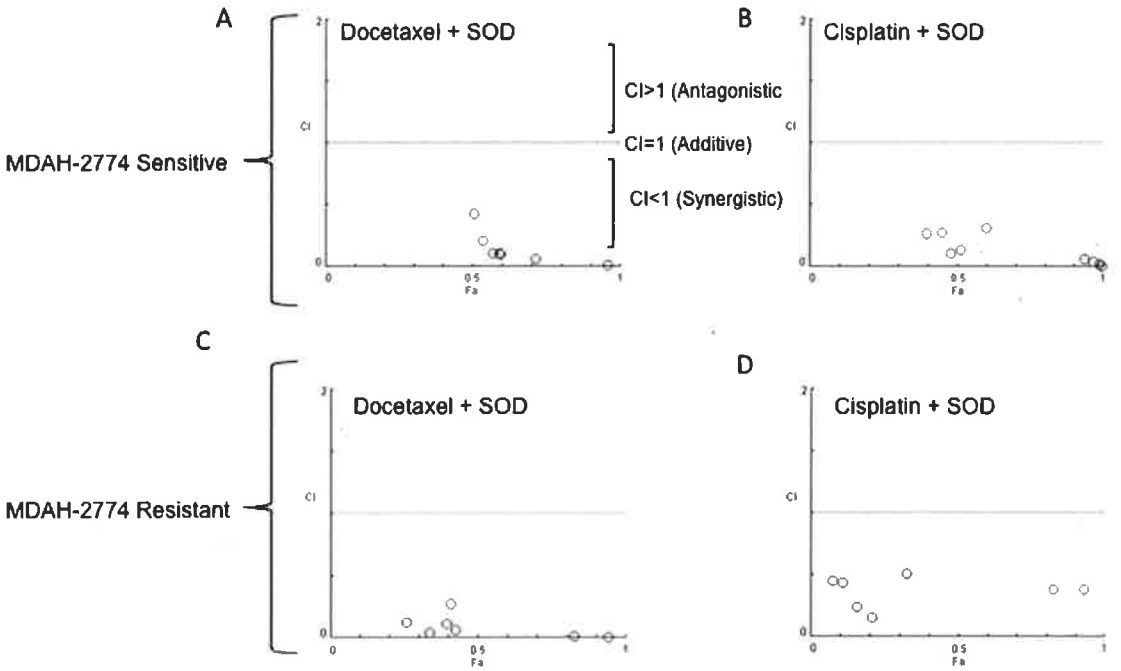

Fig. 5. SOD supplementation during chemotherapy manifested a beneficial synergistic effect. Sensitive and taxotere or cisplatin resistant MDAH-2774 cells were utilized for this experiment. Cell viability was assessed with the Vybrant MTT Cytotoxicity Assay after 24 h treatment with increasing doses of taxotere (A,C) or cisplatin (B,D) alone or in combination with SOD (10 U/ml). Taxotere/SOD (A & B) or cisplatin/SOD (C & D) combination treatments synergistically inhibited EOC cell viability as determined by Compusyn software. SOD treatment alone had no effect on cell viability. Compusyn software was utilized to generate Chou-Talalay plots (X-axis: Fa, or fractional activity, reflects the fraction of cellular viability affected by the drug treatment relative to controls; Y-axis, combination index (CI) with < 1, > 1, and $=1$ indicating synergistic, antagonistic, and additive effects, respectively). Each point represents a different combination of drug concentrations tested. Concentrations tested: taxotere (0, 0.1, 0.3, 0.6, 1.0, 2.0 3.0, 4.0 μM) or Cisplatin (0, 0.4, 0.6, 0.8, 1.0, 2.0, 3.0, 4.0 μM). Experiments were performed in triplicate. All $p < 0.05$.

specific mutation into the sensitive EOC cells, which resulted in a shift of the IC_{50} towards a higher level of chemoresistance (Fig. 4). More importantly, this mutation is known to decrease SOD activity and supplementation of SOD combined with chemotherapy in sensitive and chemoresistant EOC cells significantly increased the efficacy of the chemotherapy in a synergistic manner, with a more drastic effect in the chemoresistant cells (Figs. 5 and 6). We also observed a switch from C to T at position 242 in *CYBA* in chemoresistant as compared to their sensitive EOC cells (Table 1). Introduction of this specific mutation into the sensitive EOC cells resulted in a shift of the IC_{50} towards a lower level of chemoresistance (Fig. 4). We also observed a genotype switch from C to T at position -1040 in *GPX1* in the sensitive as compared to chemoresistant EOC cells (Table 1). Upon reversal of the SNP genotype in sensitive EOC cells, there was a shift of the IC_{50} towards a significantly higher level of chemoresistance (Fig. 4). In our chemoresistant cells lines, this genotype for *GPX1* was associated with an increase in GPX activity. Again, these findings support the notion that chemotherapy is inducing gene point mutations that happen to correspond to SNPs in locations with functional effects, thus altering overall redox balance for survival.

Recent genome-wide association studies have also successfully identified and confirmed six SNPs that appear to influence the risk of EOC [44]. The confirmed susceptibility SNPs are rs3814113 (located at 9p22, near BNC2), rs2072590 (located at 2q31, which contains a family of HOX genes), rs2665390 (located at 3q25, intronic to TIPARP), rs10088218 (located at 8q24, 700 kb downstream of MYC), rs8170 (located at 19p13, near MERIT40), and rs9303542 (located at 17q21, intronic to SKAP1) [8,44]. Recently, the CAT SNP (rs1001179) was specifically reported to be associated with increased risk for breast cancer [45]. This functional SNP, arising from a C-262T exchange on chromosome 11 in the promoter region, has been shown to decrease enzyme activity level [46]. Here, we have found an increase in mRNA and activity levels of CAT in chemoresistant as compared to sensitive EOC cells, although this specific SNP was not detected, suggesting the presence of other functional SNPs for *CAT* in EOC cells (Fig. 3). Thus, sequencing the CAT gene may reveal additional hot spot mutations that are responsible for this increase in CAT activity in chemoresistant cells. Additionally, a known functional SNP in *SOD2* (rs4880) results in a T-to-C transition at position 47 and changes the amino acid at position 16 from alanine to valine, which affects mRNA stability and impairs translocation of the precursor SOD2 protein into the mitochondrial matrix, thus reducing its activity and has been associated with increased risk of ovarian cancer [47]. In this study, we report the existence of the *SOD2* SNP (rs4880) accompanied by a decrease in SOD activity levels in the taxotere and cisplatin chemoresistant EOC cells while not in their sensitive counterparts (Table 1 and Fig. 3). Furthermore, a recent study has demonstrated that inhibition of SOD, and subsequent accumulation of $O_2^{\bullet-}$, resulted in an increase in CAT expression levels in various cancer cell lines, which is consistent with the increased CAT levels and decrease in SOD levels in chemoresistant EOC cells observed in this study (Fig. 3) [48].

Glutathione peroxidase is one of the principal antioxidant enzymes for the elimination of H_2O_2 and a key enzyme in the GSH redox cycle, resulting in the production of glutathione disulfide [14]. A nucleotide change from C to T at position -1040 in the *GPX1* gene on chromosome 3 (rs3448, also described in NCBI as position 200, 197, and 198), with unknown biological significance has been associated with increased risk of prostate cancer [49]. In this study, we observed the SNP (C/T) in sensitive EOC cells while the normal genotype (C/C) was observed in chemoresistant EOC cells (Table 1). This genotype was accompanied by an increase in GPX mRNA and activity levels in chemoresistant EOC cells as compared to their sensitive counterparts (Table 1 and Fig. 1). Again, this finding supports the notion that chemotherapy is inducing gene point mutations that happens to correspond to SNPs in locations with functional effects. The GSH redox cycle plays a central role in maintaining redox homeostasis and is a major source of protection

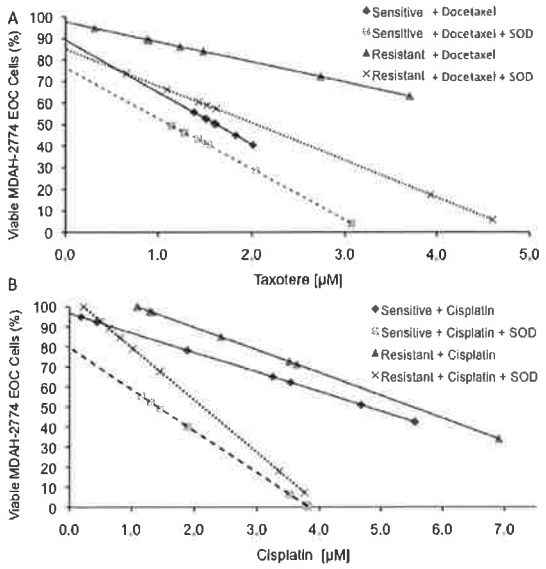

C

Predicted IC_{50}, [CI, *p<0.05]				
	Docetaxel	Docetaxel + SOD	Cisplatin	Cisplatin + SOD
MDAH-2774 Sensitive	1.62, [1.60-1.63]	1.13, [1.12-1.14]	5.50, [5.44-5.55]	1.42, [1.40-1.45]
MDAH-2774 Resistant	5.10, *[4.99-5.23]	2.04, *[2.02-2.06]	5.94, *[5.82-6.06]	2.14, *[1.93-2.34]

Fig. 6. Combination of SOD with chemotherapy increased sensitivity to chemotherapy in EOC cells. Sensitive and taxotere (A) or cisplatin (B) resistant MDAH-2774 cells were treated with chemotherapy and SOD (10 U/ml) alone or in combination for 24 h and viability was assessed with the Vybrant MTT Cytotoxicity Assay. SOD treatment alone had no effect on cell viability. The IC_{50} was predicted using regression analysis showing a beneficial shift to a lower IC_{50} upon combined treatment. 95% Confidence Intervals are listed for each treatment (C). Concentrations tested: taxotere (0, 0.1, 0.3, 0.6, 1.0, 2.0 3.0, 4.0 μM) or Cisplatin (0, 0.4, 0.6, 0.8, 1.0, 2.0, 3.0, 4.0 μM). Experiments were performed in triplicate. All $p < 0.05$.

against mild oxidative stress, while CAT becomes increasingly important in protection against severe oxidative stress, which also may explain the observed increase in CAT activity in these chemoresistant EOC cells (Fig. 3) [50]. For *GSR* (rs1002149), a G to T substitution at position 201 on chromosome 8 also affects the regulatory function of this enzyme [51]. We did not observe a *GSR* SNP in chemoresistant EOC cells although we did observe a decrease in GSR levels, again suggesting the involvement of other functional SNPs (Fig. 1).

NAD(P)H oxidase is a significant source of ROS. The membrane bound components of NAD(P)H oxidase are the catalytic subunit *CYBB* ($gp91^{phox}$) and the adjacent subunit *CYBA* ($p22^{phox}$). A specific SNP in the *CYBA* gene (rs4673), encoding the $p22^{phox}$ subunit of NAPDH oxidase, results in a C to T replacement at position 242 located on chromosome 16q24, leading to a nonconservative substitution of histidine-72 with a tyrosine [52]. This SNP is also associated with an increased risk for other diseases where oxidative stress plays a critical role in their pathophysiology, including cardiovascular disease, asthma, and diabetic nephropathy [52–54]. The mutant genotype (TT) of the *CYBA* gene has been shown to both decrease and increase activity of the protein, thereby altering the generation of $O_2^{\bullet-}$ [55–58]. Additionally, our results showed that chemoresistant cells manifested the mutant genotype for *NOS2*, another powerful proxidant enzyme, as well as an increase in iNOS levels, as compared to sensitive cells, suggests an important role for iNOS in the development of chemoresistance. The *NOS2* SNP (rs2297518) results in a change from C to T at position 2087 and has been reported to lead to higher enzymatic activity and iNOS expression, supporting the findings of our study [59]. Additionally, iNOS is an enzyme that can produce high levels of nitric oxide (NO) for prolonged periods of time; although small amounts of NO suppresses tumorigenesis by inducing apoptosis, sustained high levels of NO results in chronic inflammation [60]. In addition, it has been reported that high levels of iNOS/NO is associated with less effectiveness of platinum-based chemotherapy in breast cancer as well as resistance to cisplatin in several cancers [12,61,62].

Many chemotherapy drugs serve as a source of oxidative stress through a direct mechanism of cell death, or as an indirect effect of exposure, as observed with several chemotherapeutic agents, including the ones utilized in this study [63]. Known factors affecting the occurrence of resistance include: altered drug influx/efflux, increased cellular GSH levels, upregulation of *Bcl-2*, decreased platinum accumulation in tumor cells, increased GSH synthesis, loss of tumor necrosis factor receptor apoptosis-inducing ligand (TRAIL)-induced apoptosis, increased DNA repair and enhanced ability to repair through up-regulation of DNA repair genes. Moreover, overexpression of glutathione S-transferase is known to reduce the reactivity of various chemotherapy drugs. Additionally, loss of functional p53 augments NF-κB activated-inflammation, thus, stabilization of wild-type p53 is critical for the prevention of EOC from progression to drug-resistance [14]. Unfortunately to date, there is no known mechanism of the acquisition of chemoresistance, which is responsible for the increased mortality of this disease.

One possible explanation for the observed nucleotide switches in response to chemotherapy is nucleotide substitution, a mechanism which includes transitions, replacement of one purine by the other or that of one pyrimidine by the other, or transversions, replacement of a purine by a pyrimidine or vice versa [64]. It has been established that hydroxyl radicals react with DNA causing the formation of a large number of pyrimidine and purine-derived lesions [65]. The oxidative damage to 8-Oxo-2′-deoxyguanosine, an oxidized derivative of deoxyguanosine and major product of DNA oxidation, has been implicated in tumor initiation and progression through accumulation of genetic alterations of both oncogenes and tumor suppressor genes [65]. Indeed, previous findings revealed that GC→TA transversions derived from 8-hydroxy-2′-deoxyguanosine have been reported in the *ras* oncogene and the *p53* tumor suppressor gene in several cancers. It should be indicated however that GC→TA transversions are not unique to hydroxy-2′-deoxyguanosine, CC→TT substitutions have been identified as signature mutations for ROS [65].

Another explanation for the nucleotide switch is that chemoresistance resulted in an entirely different population of cells, with a new genotype. Chemotherapy eliminates the bulk of the tumor while leaving a core of cancer cells with high capacity for repair and renewal, known as cancer stem cells (CSCs) [66]. Tumors arising from CSCs usually contain a mixed population of cells due to the property of asymmetric division [66]. Cancer stem cells have been isolated from various types of cancer including leukemia, breast, brain, pancreatic, prostate, ovarian and colon [66]. Strikingly, CSCs were reported to be present in SKOV-3 EOC cells [67]. Additionally, CSCs have been shown to confer chemoresistance to cisplatin and doxorubicin in ovarian cancer cells [67].

Studies validating the present findings utilizing circulating tumor cells isolated from ovarian cancer patients, both sensitive and chemoresistant are currently ongoing. Additionally, the search for other hot spot point mutations in these key redox enzymes is necessary and can be established by sequencing. Here we report a novel mechanism of acquisition of chemoresistance in EOC cells which may serve as not only as the basis for future therapeutic intervention but also as potential screening tool for patients at high risk for development of chemotherapy resistance.

Author's roles

Conceptualization, N.M.F., and G.M.S.; Methodology, N.M.F., J.B., I.M., M.P.D., R.T.M, and G.M.S.; Investigation, N.M.F., I.M, and J.B.; Validation, N.M.F., J.B., and I.M.; Formal Analysis, N.M.F., J.B.,

R.T.M, and G.M.S.; Writing- Original Draft, N.M.F. and G.M.S., Writing- Review & Editing, N.M.F., J.B., I.M., M.P.D., R.T.M, and G.M.S.; Supervision, G.M.S.

Conflict of interest

The authors have declared that no conflict of interest exists.

Acknowledgements

The Wayne State University School of Medicine, Department of Obstetrics and Gynecology funds were used for this study.

Appendix A. Supplementary material

Supplementary data associated with this article can be found in the online version at doi:10.1016/j.freeradbiomed.2016.11.028.

References

[1] B.K. Erickson, M.G. Conner, C.N. Landen Jr., The role of the fallopian tube in the origin of ovarian cancer, Am. J. Obstet. Gynecol. 209 (5) (2013) 409–414.
[2] H. Kajiyama, K. Shibata, M. Mizuno, T. Umezu, S. Suzuki, R. Sekiya, K. Niimi, H. Mitsui, F. Yamamoto, M. Kawai, T. Nagasaka, F. Kikkawa, Survival benefit of taxane plus platinum in recurrent ovarian cancer with non-clear cell, non-mucinous histology, J. Gynecol. Oncol. 25 (1) (2014) 43–50.
[3] C. Lee, P. Macgregor, Drug resistance and microarrays, Mod. Drug Discov. 7 (2004) 7.
[4] J. Prat, A. Ribe, A. Gallardo, Hereditary ovarian cancer, Hum. Pathol. 36 (8) (2005) 861–870.
[5] S.J. Ramus, R.A. Vierkant, S.E. Johnatty, M.C. Pike, D.J. Van Den Berg, A.H. Wu, C.L. Pearce, U. Menon, A. Gentry-Maharaj, S.A. Gayther, R.A. Dicioccio, V. McGuire, A.S. Whittemore, H. Song, D.F. Easton, P.D. Pharoah, M. Garcia-Closas, S. Chanock, J. Lissowska, L. Brinton, K.L. Terry, D.W. Cramer, S.S. Tworoger, S.E. Hankinson, A. Berchuck, P.G. Moorman, J.M. Schildkraut, J.M. Cunningham, M. Liebow, S.K. Kjaer, E. Hogdall, C. Hogdall, J. Blaakaer, R.B. Ness, K.B. Moysich, R.P. Edwards, M.E. Carney, G. Lurie, M.T. Goodman, S. Wang-Gohrke, S. Kropp, J. Chang-Claude, P.M. Webb, X. Chen, J. Beesley, G. Chenevix-Trench, E.L. Goode, Consortium analysis of 7 candidate SNPs for ovarian cancer, Int J. Cancer 123 (2) (2008) 380–388.
[6] S.N. Teraoka, J.L. Bernstein, A.S. Reiner, R.W. Haile, L. Bernstein, C.F. Lynch, K.E. Malone, M. Stovall, M. Capanu, X. Liang, S.A. Smith, J. Mychaleckyj, X. Hou, L. Mellemkjaer, J.D. Boice Jr., A. Siniard, D. Duggan, D.C. Thomas, P. Concannon, Single nucleotide polymorphisms associated with risk for contralateral breast cancer in the Women's Environment, Cancer, and Radiation Epidemiology (WECARE) Study, Breast Cancer Res. 13 (6) (2011) R114.
[7] T.A. Sellers, Y. Huang, J. Cunningham, E.L. Goode, R. Sutphen, R.A. Vierkant, L.E. Kelemen, Z.S. Fredericksen, M. Liebow, V.S. Pankratz, L.C. Hartmann, J. Myer, E.S. Iversen Jr., J.M. Schildkraut, C. Phelan, Association of single nucleotide polymorphisms in glycosylation genes with risk of epithelial ovarian cancer, Cancer Epidemiol. Biomark. Prev. 17 (2) (2008) 397–404.
[8] S. Savas, H. Ozcelik, Phosphorylation states of cell cycle and DNA repair proteins can be altered by the nsSNPs, BMC Cancer 5 (2005) 107.
[9] J.W. Kim, C.V. Dang, Cancer's molecular sweet tooth and the Warburg effect, Cancer Res. 66 (18) (2006) 8927–8930.
[10] A. Najafov, D.R. Alessi, Uncoupling the Warburg effect from cancer, Proc. Natl. Acad. Sci. USA 107 (45) (2010) 19135–19136.
[11] E. Birben, U.M. Sahiner, C. Sackesen, S. Erzurum, O. Kalayci, Oxidative stress and antioxidant defense, World Allergy Organ J. 5 (1) (2012) 9–19.
[12] J. Belotte, N.M. Fletcher, A.O. Awonuga, M. Alexis, H.M. Abu-Soud, M.G. Saed, M.P. Diamond, G.M. Saed, The role of oxidative stress in the development of cisplatin resistance in epithelial ovarian cancer, Reprod. Sci. 21 (4) (2014) 503–508.
[13] Z. Jiang, N.M. Fletcher, R. Ali-Fehmi, M.P. Diamond, H.M. Abu-Soud, A.R. Munkarah, G.M. Saed, Modulation of redox signaling promotes apoptosis in epithelial ovarian cancer cells, Gynecol. Oncol. 122 (2) (2011) 418–423.
[14] S. Reuter, S.C. Gupta, M.M. Chaturvedi, B.B. Aggarwal, Oxidative stress, inflammation, and cancer: how are they linked?, Free Radic. Biol. Med. 49 (11) (2010) 1603–1616.
[15] J.E. Klaunig, Z. Wang, X. Pu, S. Zhou, Oxidative stress and oxidative damage in chemical carcinogenesis, Toxicol. Appl. Pharmacol. 254 (2) (2011) 86–99.
[16] R. Brigelius-Flohe, A. Kipp, Glutathione peroxidases in different stages of carcinogenesis, Biochim Biophys. Acta 1790 (11) (2009) 1555–1568.
[17] Y. Sun, Free radicals, antioxidant enzymes, and carcinogenesis, Free Radic. Biol. Med. 8 (6) (1990) 583–599.
[18] K. Buser, F. Joncourt, H.J. Altermatt, M. Bacchi, A. Oberli, T. Cerny, Breast cancer: pretreatment drug resistance parameters (GSH-system, ATase, P-glycoprotein) in tumor tissue and their correlation with clinical and prognostic characteristics, Ann. Oncol. 8 (4) (1997) 335–341.
[19] N. Saydam, A. Kirb, O. Demir, E. Hazan, O. Oto, O. Saydam, G. Guner, Determination of glutathione, glutathione reductase, glutathione peroxidase and glutathione S-transferase levels in human lung cancer tissues, Cancer Lett. 119 (1) (1997) 13–19.
[20] S.V. Singh, S.R. Brunnert, B. Roberts, A. Krishan, Differential expression of glutathione S-transferase, glutathione peroxidase and glutathione reductase in normal and malignant human breast tissues, Cancer Lett. 51 (1) (1990) 43–48.
[21] C. Di Ilio, P. Sacchetta, S. Angelucci, A. Zezza, R. Tenaglia, A. Aceto, Glutathione peroxidase and glutathione reductase activities in cancerous and non-cancerous human kidney tissues, Cancer Lett. 91 (1) (1995) 19–23.
[22] B. Popov, V. Gadjeva, P. Valkanov, S. Popova, A. Tolekova, Lipid peroxidation, superoxide dismutase and catalase activities in brain tumor tissues, Arch. Physiol. Biochem. 111 (5) (2003) 455–459.
[23] G. Ray, S. Batra, N.K. Shukla, S. Deo, V. Raina, S. Ashok, S.A. Husain, Lipid peroxidation, free radical production and antioxidant status in breast cancer, Breast Cancer Res. Treat. 59 (2) (2000) 163–170.
[24] Ho, J. Chung-man, S. Zheng, S.A. Comhair, C. Farver, S.C. Erzurum, Differential expression of manganese superoxide dismutase and catalase in lung cancer, Cancer Res. 61 (23) (2001) 8578–8585.
[25] S. Radenkovic, Z. Milosevic, G. Konjevic, K. Karadzic, B. Rovcanin, M. Buta, K. Gopcevic, V. Jurisic, Lactate dehydrogenase, catalase, and superoxide dismutase in tumor tissue of breast cancer patients in respect to mammographic findings, Cell Biochem. Biophys. 66 (2) (2013) 287–295.
[26] J. Didziapetriene, J. Bublevic, G. Smailyte, B. Kazbariene, R. Stukas, Significance of blood serum catalase activity and malondialdehyde level for survival prognosis of ovarian cancer patients, Medicina 50 (4) (2014) 204–208.
[27] J. Belotte, N.M. Fletcher, M.G. Saed, M.S. Abusamaan, G. Dyson, M.P. Diamond, G.M. Saed, A Single Nucleotide Polymorphism in Catalase Is Strongly Associated with Ovarian Cancer Survival, PLoS One 10 (8) (2015) e0135739.
[28] A.M. Svensk, Y. Soini, P. Paakko, P. Hiravikoski, V.L. Kinnula, Differential expression of superoxide dismutases in lung cancer, Am. J. Clin. Pathol. 122 (3) (2004) 395–404.
[29] Y. Hu, D.G. Rosen, Y. Zhou, L. Feng, G. Yang, J. Liu, P. Huang, Mitochondrial manganese-superoxide dismutase expression in ovarian cancer: role in cell proliferation and response to oxidative stress, J. Biol. Chem. 280 (47) (2005) 39485–39492.
[30] J.M. Malone, G.M. Saed, M.P. Diamond, R.J. Sokol, A.R. Munkarah, The effects of the inhibition of inducible nitric oxide synthase on angiogenesis of epithelial ovarian cancer, Am. J. Obstet. Gynecol. 194 (4) (2006) 1110–1116 (discussion 1116-8).
[31] G.M. Saed, N.M. Fletcher, Z.L. Jiang, H.M. Abu-Soud, M.P. Diamond, Dichloroacetate induces apoptosis of epithelial ovarian cancer cells through a mechanism involving modulation of oxidative stress, Reprod. Sci. 18 (12) (2011) 1253–1261.
[32] N.M. Fletcher, Z. Jiang, R. Ali-Fehmi, N.K. Levin, J. Belotte, M.A. Tainsky, M.P. Diamond, H.M. Abu-Soud, G.M. Saed, Myeloperoxidase and free iron levels: potential biomarkers for early detection and prognosis of ovarian cancer, Cancer Biomark 10 (6) (2011) 267–275.
[33] G.M. Saed, R. Ali-Fehmi, Z.L. Jiang, N.M. Fletcher, M.P. Diamond, H.M. Abu-Soud, A.R. Munkarah, Myeloperoxidase serves as a redox switch that regulates apoptosis in epithelial ovarian cancer, Gynecol. Oncol. 116 (2) (2010) 276–281.
[34] D.C. Castillo-Tong, D. Pils, G. Heinze, I. Braicu, J. Sehouli, A. Reinthaller, E. Schuster, A. Wolf, R. Watrowski, R.A. Maki, R. Zeillinger, W.F. Reynolds, Association of myeloperoxidase with ovarian cancer, Tumour Biol. 35 (1) (2014) 141–148.
[35] M. Lechner, P. Lirk, J. Rieder, Inducible nitric oxide synthase (iNOS) in tumor biology: the two sides of the same coin, Semin. Cancer Biol. 15 (4) (2005) 277–289.
[36] K. Roy, Y. Wu, J.L. Meitzler, A. Juhasz, H. Liu, G. Jiang, J. Lu, S. Antony, J.H. Doroshow, NADPH oxidases and cancer, Clin. Sci. 128 (12) (2015) 863–875.
[37] J. Belotte, N.M.Fletcher, A.O.Awonuga, M.Alexis, H.M.Abu-Soud, M.G.Saed, M.P. Diamond, G.M.Saed, The role of oxidative stress in the development of cisplatin resistance in epithelial ovarian cancer. Reprod. Sci., 2013.
[38] D.E. Lamendola, Z. Duan, R.Z. Yusuf, M.V. Seiden, Molecular description of evolving paclitaxel resistance in the SKOV-3 human ovarian carcinoma cell line, Cancer Res. 63 (9) (2003) 2200–2205.
[39] A.K. Godwin, A. Meister, P.J. O'Dwyer, C.S. Huang, T.C. Hamilton, M.E. Anderson, High resistance to cisplatin in human ovarian cancer cell lines is associated with marked increase of glutathione synthesis, Proc. Natl. Acad. Sci. USA 89 (7) (1992) 3070–3074.
[40] P. Zhao, Z. Zhang, H. Ke, Y. Yue, D. Xue, Oligonucleotide-based targeted gene editing in C. elegans via the CRISPR/Cas9 system, Cell Res. 24 (2) (2014) 247–250.
[41] J. Fanning, W.C. Biddle, M. Goldrosen, K. Crickard, U. Crickard, M.S. Piver, K.A. Foon, Comparison of cisplatin and carboplatin cytotoxicity in human ovarian cancer cell lines using the MTT assay, Gynecol. Oncol. 39 (2) (1990) 119–122.
[42] D. Mahalingam, E.C. Medina, J.A. Esquivel 2nd, C.M. Espitia, S. Smith, K. Oberheu, R. Swords, K.R. Kelly, M.M. Mita, A.C. Mita, J.S. Carew, F.J. Giles, S.T. Nawrocki, Vorinostat enhances the activity of temsirolimus in renal cell carcinoma through suppression of survivin levels, Clin. Cancer Res. 16 (1) (2010) 141–153.
[43] H.P. Song, S.Q. Wu, H. Hao, J. Chen, J. Lu, X. Xu, P. Li, H. Yang, A chemical family-based strategy for uncovering hidden bioactive molecules and multicomponent interactions in herbal medicines, Sci. Rep. 6 (2016) 23840.
[44] C.L. Pearce, M.A.Rossing, A.W.Lee, R.B.Ness, P.M.Webb, G.Chenevix-Trench, S.J. Jordan, D.A.Stram, J.Chang-Claude, R.Hein, S.Nickels, G.Lurie, P.J.Thompson, M. E.Carney, M.T.Goodman, K.B.Moysich, E.V.Hogdall, A.Jensen, E.L.Goode, B.L. Fridley, J.M.Cunningham, R.A.Vierkant, R.P.Weber, A.Ziogas, H.Anton-Culver, S. A.Gayther, A.Gentry-Maharaj, U.Menon, S.J.Ramus, L.A.Brinton, N.Wentzensen,

J.Lissowska, M.Garcia-Closas, L.Massuger, L.A.Kiemeney, A.M.van Altena, K.K. Aben, A.Berchuck, J.A.Doherty, E.Iversen, V.McGuire, P.G.Moorman, P.D. Pharoah, M.C.Pike, H.A.Risch, W.Sieh, D.O.Stram, K.L.Terry, A.S.Whittemore, A. Wu, J.M.Schildkraut, S.K.Kjaer, Combined and interactive effects of environmental and GWAS-identified risk factors in ovarian cancer. Cancer Epidemiol. Biomarkers Prev., 2013.

[45] S.K. Quick, P.G. Shields, J. Nie, M.E. Platek, S.E. McCann, A.D. Hutson, M. Trevisan, D. Vito, R. Modali, T.A. Lehman, M. Seddon, S.B. Edge, C. Marian, P. Muti, J.L. Freudenheim, Effect modification by catalase genotype suggests a role for oxidative stress in the association of hormone replacement therapy with postmenopausal breast cancer risk, Cancer Epidemiol. Biomark. Prev. 17 (5) (2008) 1082–1087.

[46] L. Forsberg, L. Lyrenas, U. de Faire, R. Morgenstern, A common functional C-T substitution polymorphism in the promoter region of the human catalase gene influences transcription factor binding, reporter gene transcription and is correlated to blood catalase levels, Free Radic. Biol. Med. 30 (5) (2001) 500–505.

[47] A.E. Yuzhalin, A.G. Kutikhin, Inherited variations in the SOD and GPX gene families and cancer risk, Free Radic. Res. 46 (5) (2012) 581–599.

[48] E.O. Hileman, J. Liu, M. Albitar, M.J. Keating, P. Huang, Intrinsic oxidative stress in cancer cells: a biochemical basis for therapeutic selectivity, Cancer Chemother. Pharmacol. 53 (3) (2004) 209–219.

[49] M.S. Geybels, C.M. Hutter, E.M. Kwon, E.A. Ostrander, R. Fu, Z. Feng, J.L. Stanford, U. Peters, Variation in selenoenzyme genes and prostate cancer risk and survival, Prostate 73 (7) (2013) 734–742.

[50] S. Jurkovic, J. Osredkar, J. Marc, Molecular impact of glutathione peroxidase in antioxidant processes, J. Croat. Soc. Med. Biochem. Lab. Med. 18 (2) (2008) 162–174.

[51] M. Udler, A.T. Maia, A. Cebrian, C. Brown, D. Greenberg, M. Shah, C. Caldas, A. Dunning, D. Easton, B. Ponder, P. Pharoah, Common germline genetic variation in antioxidant defense genes and survival after diagnosis of breast cancer, J. Clin. Oncol. 25 (21) (2007) 3015-3023.

[52] L. Izakovicova Holla, K. Kankova, V. Znojil, Haplotype analysis of the NADPH oxidase p22 phox gene in patients with bronchial asthma, Int Arch. Allergy Immunol. 148 (1) (2009) 73–80.

[53] A.D. Hodgkinson, B.A. Millward, A.G. Demaine, Association of the p22phox component of NAD(P)H oxidase with susceptibility to diabetic nephropathy in patients with type 1 diabetes, Diabetes Care 26 (11) (2003) 3111–3115.

[54] A. Macias-Reyes, F. Rodriguez-Esparragon, A. Caballero-Hidalgo, Y. Hernandez-Trujillo, A. Medina, J.C. Rodriguez-Perez, Insight into the role of CYBA A640G and C242T gene variants and coronary heart disease risk. A case-control study, Free Radic. Res. 42 (1) (2008) 82–92.

[55] A.A. Miller, G.R. Drummond, C.G. Sobey, Selective inhibition of NADPH-oxidase isoforms as a therapeutic strategy in hypertension, Drug Discov. Today: Ther. Strateg. 2 (3) (2005) 187–192.

[56] G. Zalba, G. San Jose, F.J. Beaumont, M.A. Fortuno, A. Fortuno, J. Diez, Polymorphisms and promoter overactivity of the p22(phox) gene in vascular smooth muscle cells from spontaneously hypertensive rats, Circ. Res. 88 (2) (2001) 217–222.

[57] Y. Shimo-Nakanishi, T. Hasebe, A. Suzuki, H. Mochizuki, T. Nomiyama, Y. Tanaka, I. Nagaoka, Y. Mizuno, T. Urabe, Functional effects of NAD(P)H oxidase p22(phox) C242T mutation in human leukocytes and association with thrombotic cerebral infarction, Atherosclerosis 175 (1) (2004) 109–115.

[58] M. Schirmer, M. Hoffmann, E. Kaya, M. Tzvetkov, J. Brockmoller, Genetic polymorphisms of NAD(P)H oxidase: variation in subunit expression and enzyme activity, Pharmacogenom. J. 8 (4) (2008) 297–304.

[59] S.S. Wang, S. Davis, J.R. Cerhan, P. Hartge, R.K. Severson, W. Cozen, Q. Lan, R. Welch, S.J. Chanock, N. Rothman, Polymorphisms in oxidative stress genes and risk for non-Hodgkin lymphoma, Carcinogenesis 27 (9) (2006) 1828–1834.

[60] F. Vannini, K. Kashfi, N. Nath, The dual role of iNOS in cancer, Redox Biol. 6 (2015) 334–343.

[61] Z. Jin, W. Wang, N. Jiang, L. Zhang, Y. Li, X. Xu, S. Cai, L. Wei, X. Liu, G. Chen, Y. Zhou, C. Liu, Z. Li, F. Jin, B. Chen, Clinical implications of iNOS levels in triple-negative breast cancer responding to neoadjuvant chemotherapy, PLoS One 10 (7) (2015) e0130286.

[62] C.H. Tang, E.A. Grimm, Depletion of endogenous nitric oxide enhances cisplatin-induced apoptosis in a p53-dependent manner in melanoma cell lines, J. Biol. Chem. 279 (1) (2004) 288–298.

[63] M. Landriscina, F. Maddalena, G. Laudiero, F. Esposito, Adaptation to oxidative stress, chemoresistance, and cell survival, Antioxid. Redox Signal. 11 (11) (2009) 2701–2716.

[64] R.L. Nussbaum, R.R. McInnes, H.F. Willard, M.W. Thompson, A. Hamosh, ScienceDirect (Online service), Thompson & Thompson Genetics in Medicine, Saunders/Elsevier, Philadelphia, 2007, p. 585.

[65] M. Sanchez, J.V. Torres, C. Tormos, A. Iradi, P. Muniz, O. Espinosa, A. Salvador, J. Rodriguez-Delgado, M. Fandos, G.T. Saez, Impairment of antioxidant enzymes, lipid peroxidation and 8-oxo-2′-deoxyguanosine in advanced epithelial ovarian carcinoma of a Spanish community, Cancer Lett. 233 (1) (2006) 28–35.

[66] A.B. Alvero, R. Chen, H.H. Fu, M. Montagna, P.E. Schwartz, T. Rutherford, D.A. Silasi, K.D. Steffensen, M. Waldstrom, L. Visintin, G. Mor, Molecular phenotyping of human ovarian cancer stem cells unravels the mechanisms for repair and chemoresistance, Cell Cycle 8 (1) (2009) 158–166.

[67] J. Chen, J. Wang, D. Chen, J. Yang, C. Yang, Y. Zhang, H. Zhang, J. Dou, Evaluation of characteristics of CD44+CD117+ ovarian cancer stem cells in three dimensional basement membrane extract scaffold versus two dimensional monocultures, BMC Cell Biol. 14 (2013) 7.